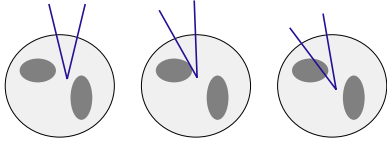


Electrical impedance tomography and Mittag-Leffler's function



Samuli Siltanen (samuli.siltanen@iki.fi)
GE Healthcare Finland

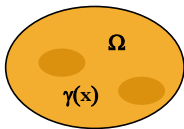
Seminar talk at Colorado State University, January 31, 2005

Acknowledgements

This is a joint work with professor **Masaru Ikehata**, Gunma University, Japan

The work was supported by
Japan Society for the Promotion of Science
(Grant-in-Aid for JSPS Fellows #00002757)

The inverse conductivity problem of Calderón



$$\Lambda_\gamma f = \gamma \frac{\partial u}{\partial \nu} \Big|_{\partial \Omega},$$

$$\begin{aligned} \nabla \cdot \gamma \nabla u &= 0 \text{ in } \Omega, \\ u &= f \text{ on } \partial \Omega. \end{aligned}$$

Uniqueness: Is the conductivity γ uniquely determined by the Dirichlet-to-Neumann (DN) map?

Reconstruction: If uniqueness holds, how to reconstruct the conductivity from the knowledge of the DN map?

The inverse conductivity problem is nonlinear

The weak formulation of the DN map as an operator

$$\Lambda_\gamma : H^{1/2}(\partial \Omega) \rightarrow H^{-1/2}(\partial \Omega),$$

is given by

$$\langle \Lambda_\gamma f, g \rangle = \int_\Omega \gamma \nabla u \cdot \nabla v,$$

where v is any H^1 function with trace g , and u satisfies the Dirichlet problem

$$\begin{cases} \nabla \cdot \gamma \nabla u = 0 & \text{in } \Omega, \\ u = f & \text{on } \partial \Omega. \end{cases}$$

Clearly, the map $\gamma \mapsto \Lambda_\gamma$ is nonlinear.

The inverse conductivity problem is ill-posed in the sense of Hadamard

Large changes in γ correspond to small changes in the DN map.

Thus, the conductivity does not depend continuously on the measurement data.

The uniqueness question in 2-D has been studied by these authors

1980 Calderón

1985 Kohn and Vogelius (piecewise real-analytic γ)

1987 Sylvester and Uhlmann ($n > 2$)

1987 R G Novikov ($n > 2$)

1988 Nachman ($n > 2$)

1996 Nachman (γ has two weak derivatives)

1997 Brown and Uhlmann (γ has one weak derivative)

2003 Astala and Päivärinta (γ essentially bounded)

**The inverse conductivity problem models
Electrical Impedance Tomography (EIT)**

Applications of EIT include

1. Medical imaging
2. Geophysical prospecting
3. Industrial process monitoring
4. Nondestructive testing

**EIT reconstruction algorithms can be divided
roughly into the following classes:**

Linearization

Iterative output least-squares methods

Statistical inversion

The inverse scattering approach, or d-bar method

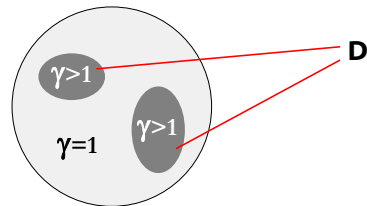
Recovery of partial information (discontinuities)

**In this talk we discuss a new EIT method for
the recovery of partial information**

We show how to use Mittag-Leffler's function to recover
discontinuities in a homogeneous background conductivity

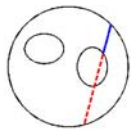
(We always take Ω to be the unit disc in the plane)

**We consider recovering an inclusion D
in homogeneous background**



**Several approaches have been suggested
to the problem of recovering inclusions**

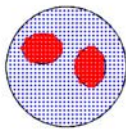
Probe method
by Ikehata



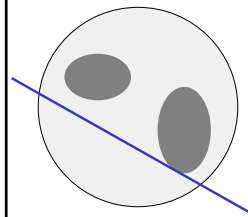
Enclosure method by
Ikehata, Ohe and Siltanen



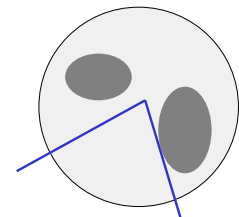
Kirsch's method
by Brühl and Hanke



**The present approach is a generalization
of the enclosure method**



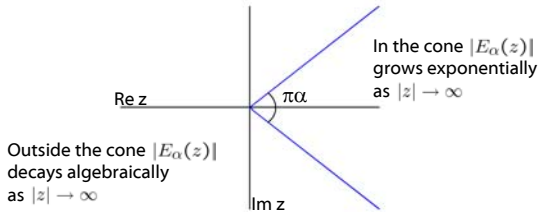
Enclosure method



Present method

**Mittag-Leffler's function:
definition and asymptotic behavior**

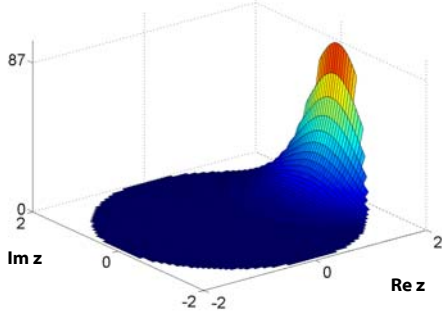
$$E_{\alpha}(z) = \sum_{m=0}^{\infty} \frac{z^m}{\Gamma(\alpha m + 1)}$$



**Mittag-Leffler's function
has a closed form expression for $\alpha=1/2$**

$$E_{1/2}(z) = e^{z^2} \left\{ 1 + \frac{2}{\sqrt{\pi}} \int_0^z e^{-u^2} du \right\}$$

**This is a plot of the absolute value
of Mittag-Leffler's function ($\alpha=1/2$ and $|z|<2$)**



**Indicator function is the key object
for recovering the inclusion from the DN map**

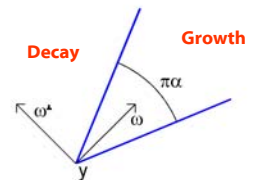
Set

$$I_{(y,\omega)}^{\alpha}(\tau) = \int_{\partial\Omega} \frac{\partial e_{\tau}^{\alpha}}{\partial \nu} (R_1 - R_{\gamma}) \frac{\partial e_{\tau}^{\alpha}}{\partial \nu} d\sigma,$$

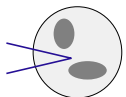
where

$$e_{\tau}^{\alpha}(x; y, \omega) = E_{\alpha}(\tau \{(x-y) \cdot \omega + i(x-y) \cdot \omega^{\perp}\}).$$

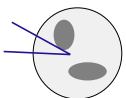
Asymptotic behavior
of e_{τ}^{α} as $|z| \rightarrow \infty$:



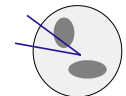
**Theorem 1: for a given cone C, we can
find out if C intersects the inclusion D**



$$\lim_{\tau \rightarrow \infty} |I_{(y,\omega)}^{\alpha}(\tau)| = 0$$



$$\liminf_{\tau \rightarrow \infty} |I_{(y,\omega)}^{\alpha}(\tau)| > 0$$



$$\lim_{\tau \rightarrow \infty} |I_{(y,\omega)}^{\alpha}(\tau)| = \infty$$

**For application of indicator function to EIT,
we must consider practical issues**

Currents are applied and voltages measured

There is a finite number of measurements

Measurements contain random errors (noise)

Measurements are done with electrodes

The parameter τ cannot be taken large

Current-to-voltage measurements are described with the ND map

The Neumann-to-Dirichlet (ND) map is defined by

$$R_\gamma f = u|_{\partial\Omega} - \frac{1}{|\partial\Omega|} \int_{\partial\Omega} u,$$

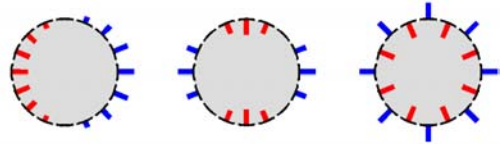
where u satisfies the Neumann problem

$$\begin{cases} \nabla \cdot \gamma \nabla u = 0 & \text{in } \Omega, \\ \gamma \frac{\partial u}{\partial \nu} = f & \text{on } \partial\Omega. \end{cases}$$

In practice, currents are applied and voltages measured. This is because the ND operator is smoothing and suppresses noise, while the DN operator is roughing and amplifies noise.

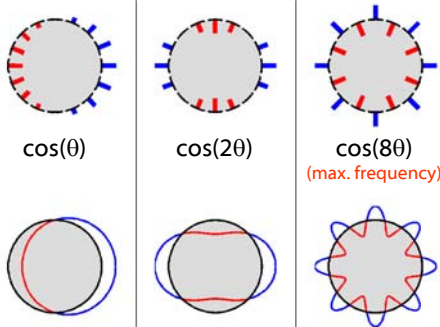
There is a finite number of linearly independent current patterns

Here are three examples with $N=16$:



Altogether, there are $N-1$ linearly independent current patterns due to conservation of charge.

We approximate the discrete currents by continuous Neumann data. Here $N=16$.



We simulate a finite set of EIT measurements with a complex 32×32 matrix

$$\text{Let } \phi_k = (2\pi)^{-1/2} (x_1 + ix_2)^k |_{\partial\Omega}, \quad k \in \mathbb{Z}.$$

We solve the Neumann problem

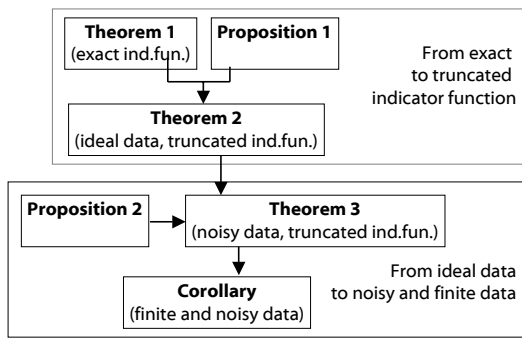
$$\nabla \cdot \gamma \nabla u_k = 0 \text{ in } \Omega, \quad \gamma \frac{\partial u_k}{\partial \nu} = \phi_k \text{ on } \partial\Omega,$$

for $k = -15, \dots, 16$. Further, we set

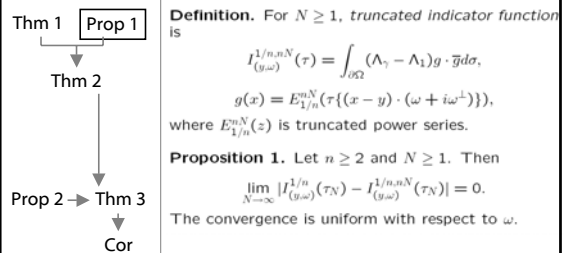
$$\mathcal{R}_\gamma [\ell, k] = \int_{\partial\Omega} u_k \overline{\phi_\ell} d\sigma,$$

and add Gaussian random numbers to the elements of \mathcal{R}_γ to simulate measurement noise.

We give extensions of Theorem 1 to cover the practical situation



Proposition 1 shows that truncated indicator function converges to the indicator function



Theorem 2 shows that the conclusion of Thm 1 holds for truncated indicator function

Thm 1 Prop 1

↓

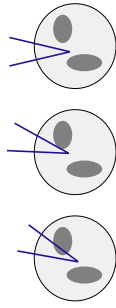
Thm 2

↓

Prop 2 → Thm 3

↓

Cor



$\lim_{N \rightarrow \infty} |I_{(y,\omega)}^{1/n,nN}(\tau_N)| = 0;$

$\liminf_{N \rightarrow \infty} |I_{(y,\omega)}^{1/n,nN}(\tau_N)| > 0;$

$\lim_{N \rightarrow \infty} |I_{(y,\omega)}^{1/n,nN}(\tau_N)| = \infty.$

Proposition 2: when noise level tends to zero, error in indicator function vanishes

Thm 1 Prop 1

↓

Thm 2

↓

Prop 2 → Thm 3

↓

Cor

Definition. Let $(y, \omega) \in \Omega \times S^1$. Define the noisy truncated indicator function by the formula

$$I_{(y,\omega)}^{1/n,nN}(\tau; \mathcal{E}^{nN}) = \sum_{0 \leq m, \ell \leq nN} \frac{\tau^{m+\ell}}{\Gamma(\frac{m}{n} + 1)\Gamma(\frac{\ell}{n} + 1)}$$

$$\times \int_{\partial\Omega} \{(\Lambda_\gamma - \Lambda_1) \{((x-y) \cdot (\omega + i\omega^\perp))^m |_{\partial\Omega} + \mathcal{E}_m^1(x)\} \cdot \{(x-y) \cdot (\omega + i\omega^\perp)\}^\ell + \mathcal{E}_\ell^2(x)\} d\sigma(x).$$

Proposition 2. Let $n \geq 2$. For $N = N(\delta; y)$ we have

$$\sup_{\|\mathcal{E}^{nN}\| \leq \delta} |I_{(y,\omega)}^{1/n,nN}(\tau_N; \mathcal{E}^{nN}) - I_{(y,\omega)}^{1/n,nN}(\tau_N)| = O(\delta^{1-\theta} |\log \delta|^{(2n-1)/n})$$

as $\delta \rightarrow 0$. The convergence is uniform with respect to ω .

Theorem 3: when noise level tends to zero, reconstruction from noisy data is possible

Thm 1 Prop 1

↓

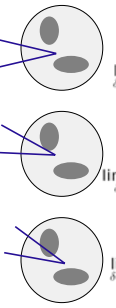
Thm 2

↓

Prop 2 → Thm 3

↓

Cor



$\limsup_{\delta \rightarrow 0} \sup_{\|\mathcal{E}^{nN}\| \leq \delta} |I_{(y,\omega)}^{1/n,nN}(\tau_N; \mathcal{E}^{nN})| = 0;$

$\liminf_{\delta \rightarrow 0} \inf_{\|\mathcal{E}^{nN}\| \leq \delta} |I_{(y,\omega)}^{1/n,nN}(\tau_N; \mathcal{E}^{nN})| > 0;$

$\liminf_{\delta \rightarrow 0} \inf_{\|\mathcal{E}^{nN}\| \leq \delta} |I_{(y,\omega)}^{1/n,nN}(\tau_N; \mathcal{E}^{nN})| = \infty.$

Corollary: when noise level tends to zero, reconstruction from finite noisy data possible

Thm 1 Prop 1

↓

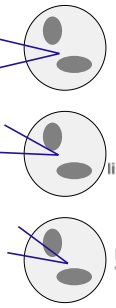
Thm 2

↓

Prop 2 → Thm 3

↓

Cor



$\limsup_{\epsilon \rightarrow 0} \sup_{\|\mathcal{E}^{nN}\| \leq \epsilon} |I_{(y,\omega)}^{1/n,nN}(\tau_N; \mathcal{E}^{nN})| = 0;$

$\liminf_{\epsilon \rightarrow 0} \inf_{\|\mathcal{E}^{nN}\| \leq \epsilon} |I_{(y,\omega)}^{1/n,nN}(\tau_N; \mathcal{E}^{nN})| > 0;$

$\liminf_{\epsilon \rightarrow 0} \inf_{\|\mathcal{E}^{nN}\| \leq \epsilon} |I_{(y,\omega)}^{1/n,nN}(\tau_N; \mathcal{E}^{nN})| = \infty.$

Indicator function can be written in terms of the measured ND map

Write $I_{(y,\omega)}^\alpha(\tau) = \int_{\partial\Omega} \frac{\partial e_\tau^\alpha}{\partial \nu} (R_1 - R_\gamma) \frac{\partial e_\tau^\alpha}{\partial \nu} d\sigma,$

and expand the function $\frac{\partial e_\tau^\alpha}{\partial \nu}$ in Fourier basis to get

$$I_{(y,\omega)}^{1/n,nN}(\tau) = 2\pi \sum_{1 \leq m, \ell \leq nN} \frac{\tau^{m+\ell} \overline{\omega^m} \omega^\ell}{\Gamma(\frac{m}{n} + 1)\Gamma(\frac{\ell}{n} + 1)}$$

$$\times \sum_{r_1=1}^m \sum_{r_2=1}^\ell \binom{m}{r_1} \binom{\ell}{r_2} r_1 r_2 (-1)^{m+\ell-r_1-r_2} y^{m-r_1} \overline{y}^{\ell-r_2}$$

$$\times (\mathcal{R}_1[r_2, r_1] - \mathcal{R}_\gamma[r_2, r_1]).$$

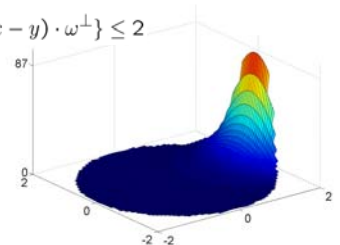
Due to the finite number of measurements, we cannot take τ to infinity

The truncated power series of Mittag-Leffler's function gives relative accuracy of 1% for $|z| < 2$. We evaluate Mittag-Leffler's function at

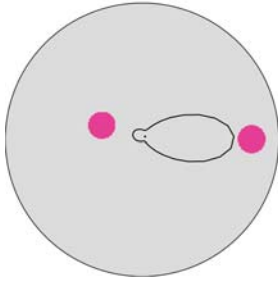
$$\tau \{(x-y) \cdot \omega + i(x-y) \cdot \omega^\perp\} \leq 2$$

Thus we choose

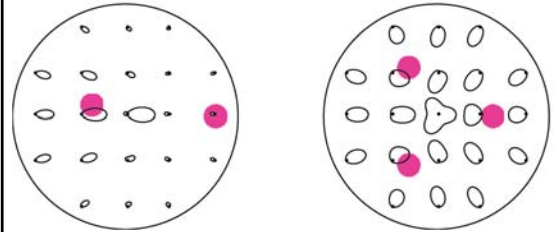
$$\tau(y) = \frac{1}{1 + |y|}$$



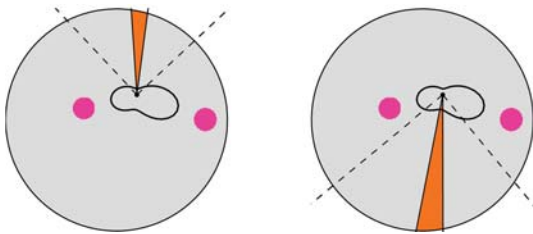
We demonstrate indicator functions by fixing y and plotting $|I(y, \omega)|$ in polar coordinates



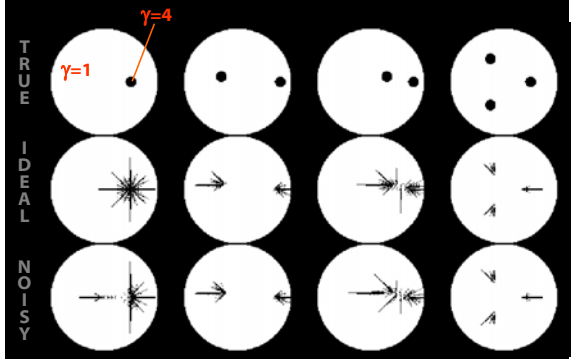
Examples of indicator functions



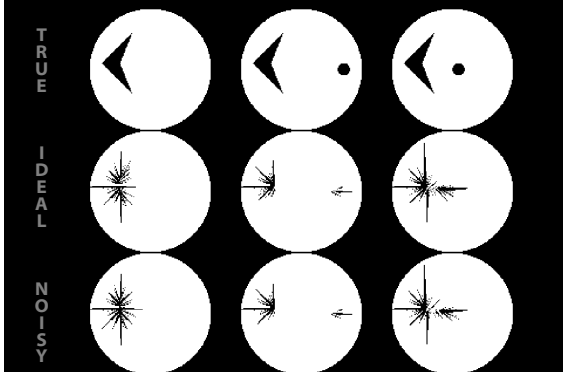
Our reconstruction strategy is to exclude cones giving local minima of the indicator function



Numerical example of recovering disc inclusions



Recovering nonconvex inclusions



References

Ikehata M and Siltanen S 2000:
Numerical method for finding the convex hull of an inclusion in conductivity from boundary measurements,
Inverse Problems **16**, pp. 1043-1052

Ikehata M and Siltanen S 2004:
Electrical impedance tomography and Mittag-Leffler's function,
Inverse Problems **20**, pp. 1325-1348